JOURNAL OF SOLID STATE CHEMISTRY **130,** 1–8 (1997)
ARTICLE NO. SC967202

Synthesis and Structure of Two New Quaternary Nitrides: $Li_3Sr_2MN_4$ (M = Nb, Ta)

X. Z. Chen and H. A. Eick[1]

Department of Chemistry and Center for Fundamental Materials Research, Michigan State University, East Lansing, Michigan 48824-1322

Received June 10, 1996; in revised form October 16, 1996; accepted October 22, 1996

Two new quaternary nitrides, $Li_3Sr_2MN_4$ (M = Nb, Ta) have been synthesized from Li, Sr, and Nb or Ta metals under a flowing Ar–NH_3 atmosphere at 800°C under ambient pressure. The structures, determined by single crystal X-ray diffraction, are orthorhombic, space group *Pnnm* (No. 58) with $Z = 4$, and have lattice parameters $a = 8.713(6)$ Å, $b = 9.007(4)$ Å, $c = 7.006(5)$ Å and $a = 8.700(6)$ Å, $b = 9.004(4)$ Å, $c = 7.000(3)$ Å for M = Nb and Ta, respectively. Refinement based upon F yielded $R = 0.033$ and $R_w = 0.036$ for M = Nb and $R = 0.035$ and $R_w = 0.045$ for M = Ta. The structures are isotypic with $Na_2Li_3MO_4$, M = Fe, Ga. The M and two independent Li atoms are tetrahedrally coordinated by N atoms. Each MN_4 tetrahedron connects three $Li(2)N_4$ tetrahedra, one by edge-sharing and two by corner-sharing, to form a two-dimensional layer in the *bc* plane. These layers are linked together by Li(1) atoms to form the three-dimensional structure. The two Sr atoms occupy channels formed by N atoms along the *c* direction. Crystalline $Li_3Sr_2NbN_4$ was synthesized by heating a Li_3N–Sr_2NbN_3 mixture at 750°C under an Ar atmosphere. Magnetic susceptibility data for $Li_3Sr_2NbN_4$ between 4 and 300 K exhibit temperature independent paramagnetism.

INTRODUCTION

Several group-V transition metal ternary nitrides have been reported recently: Ca_3VN_3 (1), M_2VN_3 (M = Ba, Sr) (2), Li_7NbN_4 (3), Li_7TaN_4 (4), $CuTaN_2$ (5), $LiTa_3N_5$ (6), $Li_{2-x}Ta_{2+x}N_4$ ($\sim 0.3 < x < \sim 1$) and $Li_{1-x}Ta_{3+x}N_4$ ($x \leq 0.06$) (7), $CsNbN_2$ (8), $NaNbN_2$ (9), $TaThN_3$ (10), Ba_2NbN_3 (11), and M_2TaN_3 (M = Ba, Sr) (12). Ba_2TaN_3 and Sr_2TaN_3 are isostructural, but Ba_2VN_3 and Sr_2VN_3 are not isostructural. Recently we reported the structures of two quaternary nitrides $Li_3Ba_2MN_4$ (M = Nb, Ta) (13) and also determined that Sr_2NbN_3 (14) is isostructural with Ba_2NbN_3 (11). These observations suggested that strontium-substituted analogs of $Li_3Ba_2MN_4$ should be preparable. However, the Guinier X-ray powder pattern for the Li_3N–Sr_2NbN_3 reaction product indexed on orthohombic symmetry with a cell volume of 548.0 Å^3, suggestive that the new Li–Sr–Nb–N phase was not an isostructural analog of monoclinic $Li_3Ba_2NbN_4$. From a comparison of the cell volumes for $Li_3Ba_2NbN_4$ (13), Ba_2NbN_3 (11), and Sr_2NbN_3 (14) which are 620.3, 954.3, and 842.4 Å, respectively, we concluded that the new Li–Sr–Nb–N phase was probably $Li_3Sr_2NbN_4$ and proceeded to try to grow a single crystal suitable for structural analysis.

Single crystals of numerous alkaline earth containing nitrides, e.g., Ca_3VN_3 (1), Ba_3MN_4 (M = Mo, W) (15), Ba_2NbN_3 (11), and $Ba_{10}[Ti_4N_{12}]$ (16), have been grown by reaction of the alkaline earth metal or metal nitride with a transition metal or metal nitride under flowing N_2(g). Sometimes Li or Li_3N was added as flux. For example, Li metal served as flux for growing crystals of Ba_2TaN_3 (12), M_3MnN_3 (M = Ba, Sr) (17), $Ba_5[CrN_4]N$ (18), and $Li_3Ba_2MN_4$ (M = Nb, Ta) (13). Other methods of crystal growth include: (i) synthesis of Ca_3CrN_3 (19) by heating a mixture of CrN/Cr_2N and Ca_3N_2 in a stainless-steel tube under an Ar atmosphere, (ii) synthesis of Sr_2NiN_2 (20) by using a nonreactive Na metal flux, and (iii) synthesis of numerous alkali metal containing nitrides under high pressure by using alkali metal amides as the nitrogen source (21).

We decided to try to grow single crystals of $Li_3Sr_2MN_4$ (M = Nb, Ta) under flowing NH_3(g) under ambient pressure. Since ammonia is a more reactive nitriding reagent than N_2(g), we hoped to obtain crystals at lower temperatures than those required in an N_2(g) atmosphere. To our knowledge, crystals of transition metal nitrides had not been grown under flowing ammonia under ambient pressure.

Very few quaternary transition metal nitrides have been reported. Most of those reported involve Li–M–Ni–N (M = Ca, Sr, or Ba) systems (22). In $LiSr_2CoN_2$ (23) and $M_2LiFe_2N_3$ (M = Ba or Sr) (24), $[Co^IN_2]^{5-}$ and $[Fe_2N_3]^{5-}$ anions, respectively, were characterized. We report the synthesis and structures of the quaternary nitrides, $Li_3Sr_2MN_4$ (M = Nb, Ta).

[1] To whom correspondence should be addressed.

0022-4596/97 $25.00

EXPERIMENTAL

Synthesis. Polycrystalline $Li_3Sr_2NbN_4$ was synthesized by heating at 750°C for 30 h a mixture of Li_3N and Sr_2NbN_3 (14). The 1 : 1 molar ratio mixture with a $\sim 10\%$ excess of Li_3N was sealed in a Nb tube under an Ar atmosphere. Previously unreported Sr_2NbN_3 was synthesized by heating a 1 : 1 molar mixture of Sr_2N (25) and NbN at 900°C for 1 day under flowing NH_3(g) followed by quenching. Sr_2N was prepared by heating Sr metal in flowing N_2(g) at 800°C for 36 h. NbN was prepared by heating $NbCl_5$ (Johnson Matthey, grade 1) under flowing NH_3(g) to 700°C in 3 h, heating it at 700°C for 8 h, and then quenching.

Single crytals of $Li_3Sr_2NbN_4$ were grown from Li, Sr, and Nb metals. A mixture of elemental Li, Sr (99%, Cerac, Inc.), and Nb powder (99%, E. H. Sargent & Co., 80 mesh) in 3 : 1.5 : 1 molar ratio was confined in a Nb boat which was then placed in a quartz reaction tube. The mixture was first heated under flowing Ar (AGA Gas, Inc.) to 800°C at a rate of 110°C/h and held at this temperature under flowing Ar for about 40 min. NH_3(g) was then slowly diffused into the Ar-filled reaction system. The sample was heated under the flowing Ar/NH_3(g) mixture for 29 h. The volume ratio of Ar(g) and NH_3(g) was maintained between approximately 1 : 1 and 3 : 2. The sample was next heated at 800°C under flowing Ar for 5 h and finally cooled to 200°C under flowing Ar at a rate of 10°C/h. To ensure that the NH_3(g) was dry, Sr metal was placed before and after the sample. Light-yellow transparent single crystals of $Li_3Sr_2NbN_4$ were isolated from the crushed product which was both air and moisture sensitive.

The argon gas was purified by molecular sieves (4–8 mesh, Aldrich) and De-Ox catalyst (Johnson Matthey). The ammonia was dried over sodium metal and stored in a stainless-steel vessel. All sample manipulations were handled in an Ar-filled glove box the typical moisture and oxygen contents of which were < 0.5 ppm$_v$ and < 1 ppm$_v$, respectively. Single crystals of $Li_3Sr_2TaN_4$ were grown similarly with minor changes to the heating schedule.

X-ray diffraction. X-ray powder diffraction data were obtained by using both a 114.6 mm Guinier camera (quartz monochromatized Cu$K\alpha_1$ radiation) and Philips APD powder diffractometer system (graphite monochromatized Cu$K\alpha$ radiation) with a Philips XRG-3000 X-ray generator. The diffractometer data were stripped of the $K\alpha_2$ component with the APD software and corrected for the θ-compensating slit as described previously (26). The programs VISSER (27), TREOR5 (28), and DICVOL92 (29) were used to index the Guinier X-ray powder pattern of $Li_3Sr_2NbN_4$. NBS certified Si ($a = 5.43082(3)$ Å) served as internal standard. The program LAZY PULVERIX (30) was used for intensity calculations. X-ray single crystal diffraction data were collected on a Rigaku AFC6S four-circle diffractometer.

Structure determination. Irregular crystals for both compounds were selected and sealed in glass capillaries in an N_2-filled glove bag. Lattice parameters were obtained by least-squares refinement of the angle settings of 20 carefully centered reflections. The choice of space groups was reduced to *Pnnm* (No. 58) and *Pnn*2 (No. 34) by systematic absences ($0kl$, $k + l \neq 2n$; $h0l$, $h + l \neq 2n$), and the structures were solved based on space group *Pnnm*.

Data were collected at room temperature by the ω–2θ scan technique to $2\theta \leq 60°$. The intensities of three representative reflections measured after every 150 reflections declined by 3.70% and 0.5% for M = Nb and Ta, respectively. A linear correction factor was applied to correct for this intensity loss. The linear absorption coefficient for Mo$K\alpha$ radiation was used in the program DIFABS to make an empirical absorption correction which resulted in transmission factors that ranged from 0.66 to 1.33 and from 0.86 to 1.16 for the M = Nb and Ta compounds, respectively (31). The data were corrected for Lorentz and polarization effects and for secondary extinction (coefficients = $0.2 \pm 0.1 \times 10^{-6}$ and $0.51 \pm 0.08 \times 10^{-6}$, respectively).

TABLE 1
Summary of Crystal and Diffraction Data for $Li_3Sr_2MN_4$ (M = Nb, Ta)

Chemical formula	$Li_3Sr_2NbN_4$	$Li_3Sr_2TaN_4$
Formula weight	345.00	433.04
Space group	*Pnnm* (No. 58)	*Pnnm* (No. 58)
a (Å)	8.713(6)	8.700(6)
b (Å)	9.007(4)	9.004(4)
c (Å)	7.006(5)	7.000(3)
V (Å^3)	550(1)	548.3(5)
Z	4	4
D_{calc} (g/cm^3)	4.167	5.245
T (°C)	26 ± 1	25 ± 1
Crystal color, Habit	light yellow, irregular	light yellow, irregular
Crystal dimensions (mm)	$0.150 \times 0.200 \times 0.300$	$0.140 \times 0.100 \times 0.140$
2θ max (deg)	60.0	60.0
Scan type	ω–2θ	ω–2θ
X-ray radiation (λ)	Mo$K\alpha$ ($\lambda = 0.71069$ Å)	Mo$K\alpha$ ($\lambda = 0.71069$ Å)
Monochromator	Graphite	Graphite
Octants collected	hkl; $\overline{hkl}$	hkl
Absorption coeff μ(cm^{-1})	205.98	383.64
Measured reflections	1952	965
Observed reflections[a]	408	617
Unique reflections	970	861
$F000$	616	744
No. of variables	55	55
Residue peaks	1.81 (-1.49) e$^-$/Å^3	3.84 (-2.16) e$^-$/Å^3
R^b, R_w^c	0.033, 0.036	0.035, 0.045

[a] $I > 3.00\sigma(I)$.
[b] $R = \sum \| F_0 \| - |F_c| / \sum |F_0|$.
[c] $R_w = [(\sum w(|F_0| - |F_c|)^2 / \sum w F_0^2)]^{1/2}$.

TABLE 2
Atomic Positional and B_{eq} Parameters for $Li_3Sr_2MN_4$ (M = Nb, Ta)

Atom	Position	x	y	z	B_{eq} (Å^2)[a]
Li(1)	8(*h*)	0.017(2)	0.363(2)	0.236(2)	1.0(7)
		0.018(2)	0.363(2)	0.238(3)	0.5(7)
N(1)	8(*h*)	0.302(1)	0.0205(8)	0.234(1)	1.1(4)
		0.303(1)	0.019(1)	0.234(1)	0.5(3)
N(2)	4(*g*)	0.073(2)	0.220(1)	0	0.7(5)
		0.075(2)	0.219(2)	0	1.0(6)
Li(2)	4(*g*)	0.206(4)	0.425(2)	0	1.(1)
		0.208(5)	0.426(4)	0	1.(1)
Sr(1)	4(*g*)	0.2423(2)	0.7542(2)	0	1.02(6)
		0.2418(2)	0.7543(2)	0	0.76(6)
Nb	4(*g*)	0.2855(2)	0.1368(1)	0	0.45(5)
Ta		0.28558(7)	0.13711(7)	0	0.15(2)
N(3)	4(*g*)	0.451(2)	0.284(1)	0	1.0(5)
		0.452(2)	0.284(2)	0	0.6(5)
Sr(2)	4(*e*)	0	0	0.2602(2)	0.67(5)
		0	0	0.2603(2)	0.38(5)

Note. Each first line is for M = Nb; each second line is for M = Ta.
[a] The equivalent isotropic temperature factor is defined as (41)

$$B_{eq} = \frac{8\pi^2}{3}\left[\sum_{i=1}^{3}\sum_{j=1}^{3} U_{ij}a_i^* a_j^* \mathbf{a}_i\mathbf{a}_j\right].$$

TABLE 3
Anisotropic Thermal Parameters, U_{ij} (×1000)[a] for $Li_3Sr_2MN_4$

Atom	U_{11}	U_{22}	U_{33}	U_{12}	U_{13}	U_{23}
Li(1)	10(10)	13(7)	12(8)	0(1)	− 3(8)	− 0(10)
	20(10)	− 11(7)	10(10)	2(7)	− 4(8)	− 3(8)
N(1)	16(5)	17(4)	9(4)	5(4)	0(5)	4(4)
	3(4)	13(4)	4(4)	− 3(3)	− 0(4)	0(4)
N(3)	4(7)	19(6)	15(7)	4(5)	0	0
	1(6)	15(7)	8(7)	− 5(5)	0	0
Li(2)	20(20)	10(10)	10(10)	− 0(10)	0	0
	50(20)	0(10)	− 0(10)	10(20)	0	0
Sr(1)	11.7(8)	11.2(7)	15.9(8)	− 2.2(5)	0	0
	8.8(7)	6.6(8)	13.4(8)	− 2.6(5)	0	0
Nb	5.8(6)	6.8(6)	4.4(5)	0.8(6)	0	0
Ta	2.2(3)	2.1(3)	1.3(3)	0.2(3)	0	0
N(2)	17(8)	11(6)	0(6)	− 1(5)	0	0
	5(7)	2(6)	30(10)	5(5)	0	0
Sr(2)	9.3(8)	9.4(5)	6.7(6)	1.5(6)	0	0
	4.7(6)	5.9(6)	3.7(7)	0.6(5)	0	0

Note. Each first line is for M = Nb; each second line is for M = Ta.
[a] The anisotropic temperature factor coefficients U_{ij} are defined as

$$\exp(-2\pi^2(a^{*2}U_{11}h^2 + b^{*2}U_{22}k^2 + c^{*2}U_{33}l^2 + 2a^*b^*U_{12}hk + 2a^*c^*U_{13}hl + 2b^*c^*U_{23}kl)).$$

Both structures were solved by direct methods with the program SHELXS86 (32). Except as described below, all atoms were refined anisotropically with the refinement based upon F. For $Li_3Sr_2TaN_4$, N(2) and two Li atoms could not be refined anisotropically, presumably because of crystal imperfections.

Neutral atoms scattering factors were taken from Cromer and Waber (33). All calculations were performed with the TEXSAN (34) crystallographic software package. Data collection and atomic position parameters are listed in Tables 1 and 2, respectively. Thermal parameters (U_{ij}) are presented in Table 3. See NAPS document No. 05356 for 22 pages or 1 fiche of supplementary material.[2]

[2] This is not a multi-article document. Order from NAPS c/o Microfiche Publications, P.O. Box 3513, Grand Central Station, New York, NY 10163-3513. Remit in advance in U.S. funds only $8.35 for photocopies or $5.00 for microfiche. There is a $15.00 invoicing charge on all orders filled before payment. Outside U.S. and Canada add postage of $4.50 for the first 20 pages and $1.00 for each 10 pages of material thereafter, or $1.75 for the first microfiche and 50¢ for each microfiche thereafter.

Magnetic susceptibility. Data were measured with a Quantum Design SQUID magnetometer at temperatures between 4 and 300 K. Since magnetic susceptibilities are slightly field dependent measurements were also performed at various magnetic fields between 200 and 6000 G and the susceptibilities at fields of 200, 400, and 600 G were extrapolated to zero reciprocal field to eliminate ferromagnetic impurity contributions.

RESULTS AND DISCUSSION

Both light-yellow and air sensitive $Li_3Sr_2MN_4$ compounds decompose in air within minutes with release of ammonia. In the synthesis of polycrystalline $Li_3Sr_2NbN_4$ too great an excess of Li_3N and too high a reaction temperature may lead to formation of $Li_{16}Nb_2N_8O$ (35) unless the reactants and Ar atmosphere are absolutely oxygen-free.

The volume ratio of Ar(g) to NH_3(g) was thought to be critical for the crystal growth and was controlled carefully in order to maintain mild reaction conditions. The advantage of growing nitride crystals under flowing NH_3(g) instead of flowing N_2(g) is that the reaction can be carried out at a lower temperature. Use of NH_3(g) may allow many reactions which are otherwise difficult or impossible under

flowing N_2(g) to proceed. Li metal reacts readily with NH_3(g) to form a low-melting amide (melting point, 380°C) (36) which allows the reaction to proceed in the liquid state. The reaction temperature, however, must not be too high since $LiNH_2$ vaporizes at elevated temperatures.

$Li_3Sr_2NbN_4$ and $Li_3Sr_2TaN_4$ crystalline isotypically with $Na_2Li_3FeO_4$ (37) and $Na_2Li_3GaO_4$ (38). The crystal structure of $Li_3Sr_2NbN_4$ is shown in Figs. 1 and 2. Selected bond distances and angles for both structures are given in Table 4. The layer structure is shown in Fig. 1 with the Li(1) and Sr atoms omitted for clarity. As shown in Fig. 2, the Nb and Li(2) atoms are tetrahedrally coordinated by N atoms. Each NbN_4 tetrahedron connects three Li(2)N_4 tetrahedra, one by edge sharing and two by corner sharing, to form

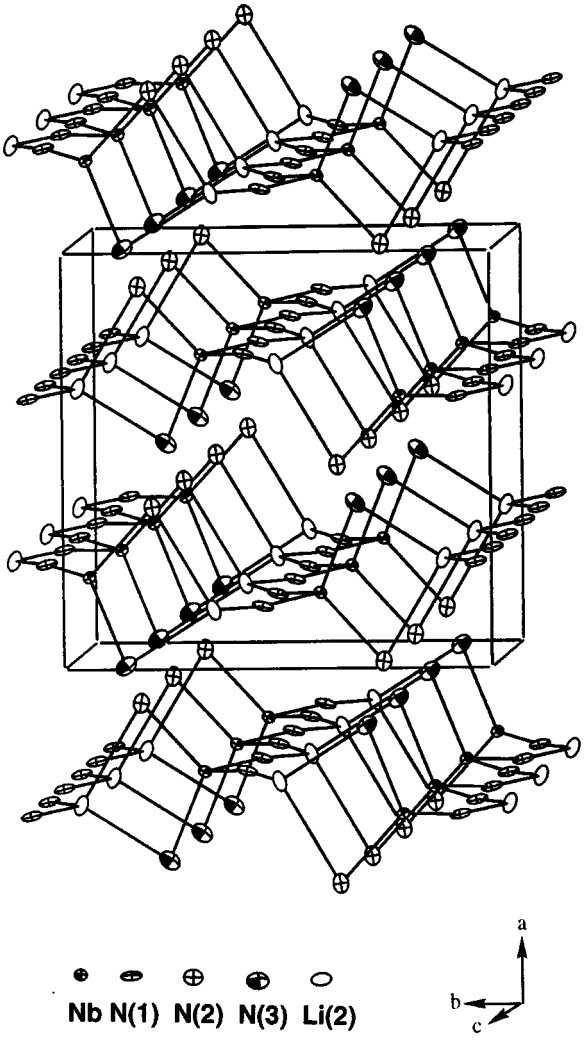

FIG. 1. NbN_4 and Li(2)N_4 tetrahedra in $Li_3Sr_2NbN_4$ share edges and corners with each other to form layers in the *bc* plane. The Li(1), Sr(1), and Sr(2) atoms are omitted for clarity.

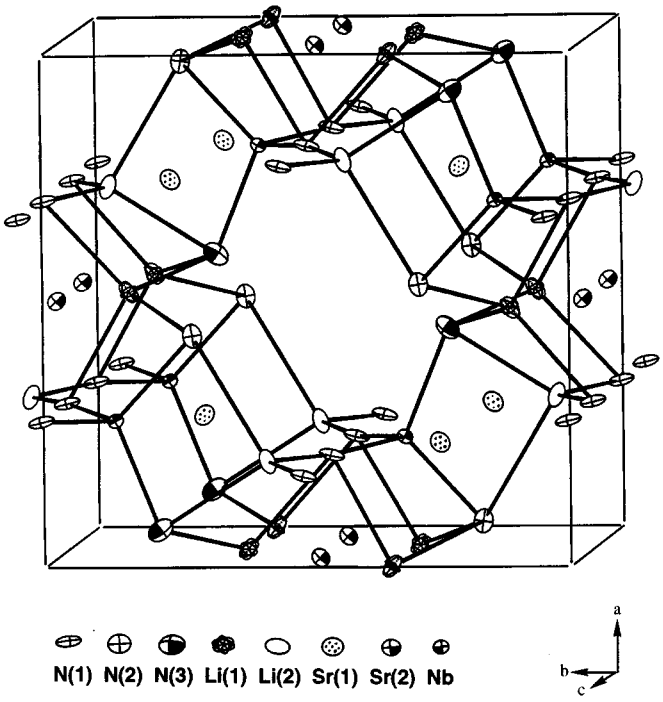

FIG. 2. The structure of $Li_3Sr_2NbN_4$ showing the layers of Li(2)N_4 and NbN_4 tetrahedra in the *bc* plane linked by Li(1) atoms. Strontium atoms are located in channels in the structure.

a two-dimensional layer in the *bc* plane. A mirror plane which crosses over atoms Nb, Li(2), N(3), and N(2) can be detected from the sum of the four bond angles, N(2)–Nb–N(3) (115.4°), N(2)–Li(2)–N(3) (91.5°), Nb–N(3)–Li(2) (73.4°), and Nb–N(2)–Li(2) (79.7°), which total 360°. A similar situation prevails for the Li(2), Fe, O(2), and O(3) atoms in $Na_2Li_3FeO_4$, where the comparable angles also sum to 360° (37). The *X*–Li–*X* angles of the Li-atom tetrahedra in these nitrides are compared in Table 5 with those of the corresponding tetrahedra in $Na_2Li_3FeO_4$. The *X*–Li(2)–*X*, *X*=O, tetrahedra is slightly less distorted than the corresponding *X*=N tetrahedra with the reverse situation prevailing for the Li(1) tetrahedra.

The average bond distances for Nb–N and Li(2)–N in $Li_3Sr_2NbN_4$ are 1.97 and 2.24 Å, respectively, close to those in $Li_3Ba_2NbN_4$ which has an Nb–N distance of 1.95 Å and an average Li–N distance of 2.18 Å. The Nb–N bond distance reported for Li_7NbN_4, where the Nb atoms are also tetrahedrally coordinated by N atoms, is also 1.95 Å (3). The average Ta–N bond distance in $Li_3Sr_2TaN_4$ is 1.96 Å, close to that in $Li_3Ba_2TaN_4$ which has an average Ta–N distance of 1.95 Å. The tetrahedrally coordinated Li(2) in $Li_3Sr_2TaN_4$ has Li(2)–N distances of 2.05, 2.19, and 2.48 Å (average 2.24 Å), comparable to the Li(1)–N distances which range between 2.21 and 2.43 Å (average 2.32 Å) in $Li_3Ba_2TaN_4$.

TABLE 4
Selected Bond Distance (Å) and Angles (deg) in $Li_3Sr_2MN_4$, M = Nb, Ta

Bond distances				Bond angles			
	M = Nb	M = Ta			M = Nb	M = Ta	
M–N(3)	1.96(1)	1.96(2)		N(1)–M–N(3)	107.9(3)	108.1(4)	(2×)
M–N(1)	1.953(8)	1.96(1)	(2×)	N(2)–M–N(3)	115.4(6)	115.7(6)	
M–N(2)	2.00(1)	1.97(2)		N(1)–M–N(1)	114.5(5)	113.3(6)	
Li(1)–N(3)	2.35(2)	2.33(2)		N(1)–M–N(2)	105.7(3)	105.9(6)	(2×)
Li(1)–N(1)	2.15(2)	2.16(2)		N(1)–Li(1)–N(3)	89.2(8)	89.7(9)	
	2.13(2)	2.11(2)			118.6(9)	119.(1)	
Li(1)–N(2)	2.15(2)	2.17(2)		N(2)–Li(1)–N(3)	108.8(7)	108.8(8)	
Li(2)–N(3)	2.48(3)	2.48(4)		N(1)–Li(1)–N(1)	108.1(7)	107.7(7)	
Li(2)–N(1)	2.05(1)	2.05(2)	(2×)	N(1)–Li(1)–N(2)	124.2(9)	124.(1)	
Li(2)–N(2)	2.18(3)	2.19(4)			107.8(9)	107.(1)	
Sr(1)–N(3)	2.70(1)	2.69(1)		N(1)–Li(2)–N(3)	104.3(9)	104.(1)	(2×)
Sr(1)–N(1)	2.954(8)	2.94(1)	(2×)	N(2)–Li(2)–N(3)	91.5(9)	91.(1)	
	2.836(8)	2.85(1)	(2×)	N(1)–Li(2)–N(1)	130.(1)	131.(1)	
Sr(1)–N(2)	2.75(1)	2.77(2)		N(1)–Li(2)–N(2)	109.6(9)	109.(1)	(2×)
Sr(2)–N(3)	2.608(9)	2.60(1)	(2×)	N(1)–Sr(1)–N(3)	85.8(3)	85.7(3)	(2×)
Sr(2)–N(1)	2.65(1)	2.65(1)	(2×)		92.4(3)	92.3(3)	(2×)
Sr(2)–N(2)	2.767(9)	2.76(1)	(2×)	N(1)–Sr(1)–N(1)	67.6(3)	67.7(4)	
M–Sr(1)	3.466(3)	3.468(2)			172.7(2)	172.8(4)	(2×)
M–Sr(2)	3.321(2)	3.319(2)	(2×)		105.21(6)	105.28(6)	(2×)
M–Li(1)	2.74(2)	2.73(2)	(2×)		81.9(2)	81.7(4)	
M–Li(2)	2.68(2)	2.68(3)		N(1)–Sr(1)–N(2)	96.2(3)	96.3(3)	(2×)
Sr(1)–Li(1)	2.97(2)	2.95(2)	(2×)		85.8(3)	86.0(3)	(2×)
	2.99(2)	3.00(2)	(2×)	N(3)–Sr(2)–N(3)	99.8(4)	99.8(4)	
Sr(1)–Li(2)	2.98(2)	2.97(3)		N(1)–Sr(2)–N(3)	99.0(3)	99.0(4)	(2×)
Sr(2)–Li(1)	3.28(2)	3.28(2)	(2×)		86.1(3)	86.2(4)	(2×)
Sr(2)–Li(2)	3.13(3)	3.12(4)	(2×)	N(2)–Sr(2)–N(3)	85.8(2)	86.0(3)	(2×)
Li(1)–Li(1)	2.48(3)	2.49(3)			157.2(4)	157.0(4)	(2×)
Li(1)–Li(2)	2.40(3)	2.41(4)		N(1)–Sr(2)–N(1)	172.2(4)	171.9(5)	
				N(1)–Sr(2)–N(2)	71.2(3)	70.8(4)	(2×)
					103.5(3)	103.6(4)	(2×)
				N(2)–Sr(2)–N(2)	97.6(3)	97.5(4)	
				M–N(3)–Li(2)	73.4(7)	73.4(9)	
				M–N(2)–Li(2)	79.7(9)	80.(1)	

TABLE 5
A Comparison between the X–Li–X Bond Angles of $Na_2Li_3FeO_4$ (X=O) and $Li_3Sr_2NbN_4$ (X=N)

Bond angle	X=O	X=N	
X(1)–Li(1)–X(3)	119.5(7)	118.6(9)	
	92.5(6)	89.2(8)	
X(2)–Li(1)–X(3)	117.0(8)	108.8(7)	
X(1)–Li(1)–X(1)	101.9(7)	108.1(7)	
X(1)–Li(1)–X(2)	120.1(7)	124.2(9)	
	105.2(7)	107.8(9)	
X(1)–Li(2)–X(3)	110.2(6)	104.3(9)	(2×)
X(2)–Li(2)–X(3)	96.(1)	91.5(9)	
X(1)–Li(2)–X(2)	103.5(7)	109.6(9)	

The layers formed by the Nb and Li(2)–N tetrahedra are linked together by Li(1) atoms, also tetrahedrally coordinated by N atoms, to form the three-dimensional structure (Fig. 1). The average Li–N distance of 2.22 Å in $Li_3Sr_2NbN_4$ is larger than that in $Li_3Ba_2NbN_4$ because one of the two independent Li atoms in the latter case is threefold coordinated by N atoms. The threefold coordinated Li–N distance in Li_3N is 2.106 Å (39).

The two Sr atoms occupy the channels formed by N atoms along the c direction (Fig. 2). Their coordination environments are shown in Fig. 3; Sr–N distances range from 2.608 to 2.954 Å. The resultant octahedra are distored based on the bond angles presented in Table 4. Figure 4 shows the coordination environments for N atoms which are similar to that of the N(3) atom in Ba_3MoN_4 (15).

The $Li_3Sr_2MN_4$ structures share some common features with the previously reported nitrides $Li_3Ba_2MN_4$ (M = Nb, Ta) (13). In the $Li_3Ba_2MN_4$ structures, Nb and Ta atoms and one of two independent Li atoms are also tetrahedrally coordinated by N atoms. Both compounds have a basic structure unit in which one MN_4 tetrahedron connects with one LiN_4 tetrahedron by edge sharing. Each MN_4 tetrahedra in $Li_3Ba_2MN_4$ however, only connects two, not three, $Li(2)N_4$ tetrahedra to form a one-dimensional chain, not a layer as in $Li_3Sr_2MN_4$ (M = Nb, Ta).

Lattice parameters derived by least squares refinement (40) of data obtained by the Guinier technique (internal standard: NBS certified Si, $a_0 = 5.43094(3)$ Å) were $a = 8.705(1)$ Å, $b = 9.000(2)$ Å, and $c = 6.997(1)$ Å. Observed and calculated d spacings and intensities are given in Table 6. The magnetic susceptibility of $Li_3Sr_2NbN_4$ exhibits

TABLE 6
Miller Indices and Observed and Calculated Interplanar Distances and Intensities for $Li_3Sr_2NbN_4$

h	k	l	d_o	d_c[a]	I_o	I_c	h	k	l	d_o	d_c[a]	I_o	I_c
1	1	0	6.2729	6.2624	19	51	4	2	2		1.7111		27
0	1	1	5.5362	5.5300	15	33	1	5	1	1.7100	1.7107	33	21
2	0	0	4.3564	4.3565	10	20	4	3	1		1.7098		3
1	2	0	4.0075	4.0007	22	39	2	3	3	1.6970	1.6976	5	8
0	0	2	3.5050	3.5030	8	14	1	1	4	1.6874	1.6868	2	3
2	1	1	3.4241	3.4221	14	26	1	2	4	1.6040	1.6045	3	5
2	2	0	3.1314	3.1312	31	51	4	4	0	1.5648	1.5656	4	4
1	1	2	3.0568	3.0572	18	32	3	3	3	1.5557	1.5563	6	12
2	2	1	2.8585	2.8587	3	5	5	1	2	1.5356	1.5373	6	9
1	3	0	2.8392	2.8385	16	16	3	5	0		1.5308		2
0	2	2		2.7650	100	100	2	2	4	1.5279	1.5286	7	13
3	1	0	2.7637	2.7642		40	5	3	0	1.5059	1.5071	4	6
0	3	1		2.7596		15	4	2	3	1.4990	1.5017	3	4
2	0	2	2.7290	2.7299	65	95	3	5	1	1.4944	1.4956	11	13
1	2	2		2.6355	50	20	1	3	4	1.4883	1.4906	3	4
1	3	1	2.6318	2.6308		56	3	1	4	1.4784	1.4795	6	9
2	1	2	2.6080	2.6126	3	4	1	6	0		1.4794		2
3	1	1	2.5614	2.5713	8	8	5	3	1	1.4717	1.4734	3	4
3	2	0	2.4409	2.4408	7	7	2	6	0	1.4187	1.4193	3	3
2	3	1	2.3319	2.3313	9	13	3	4	3		1.4154		1
0	1	3	2.2606	2.2606	3	5	1	5	3	1.4065	1.4076	7	11
0	4	0	2.2516	2.2517	5	6	3	5	2	1.4009	1.4027	3	6
1	3	2	2.2055	2.2054	8	13	0	4	4	1.3807	1.3825	6	2
4	0	0	2.1782	2.1783	19	28	6	2	0		1.3821		7
3	1	2	2.1675	2.1700	3	6	4	0	4	1.3635	1.3650	7	11
3	2	2		2.0026		5	1	6	2		1.3628		5
3	3	1	2.0005	2.0005	25	29	6	2	1	1.3545	1.3560	2	3
2	4	0		2.0003		4	5	4	1	1.3503	1.3522	3	3
0	4	2	1.8928	1.8942	4	5	4	1	4		1.3496		2
4	2	1	1.8866	1.8883	5	9	3	3	4	1.3402	1.3418	5	1
4	0	2	1.8496	1.8498	2	1	6	0	2		1.3415		8
0	3	3	1.8414	1.8433	2	3	2	1	5	1.3182	1.3195	1	3
3	0	3	1.8178	1.8200	2	1	2	4	4	1.3166	1.3177	2	2
4	1	2	1.8102	1.8120	3	4	3	5	3	1.2792	1.2803	5	8
1	3	3	1.8019	1.8034	11	17	5	3	3	1.2649	1.2663	2	2
3	3	2	1.7923	1.7932	19	26	1	3	5	1.2552	1.2565	3	5
3	1	3	1.7825	1.7839	1	2	5	5	0		1.2525		2
1	5	0	1.7626	1.7641	4	6	3	6	2	1.2414	1.2463	2	2
0	0	4	1.7511	1.7515	12	23	1	5	4		1.2429		3
3	4	1	1.7232	1.7248	4	5							

[a] Calculated from lattice parameters listed in Table 1.

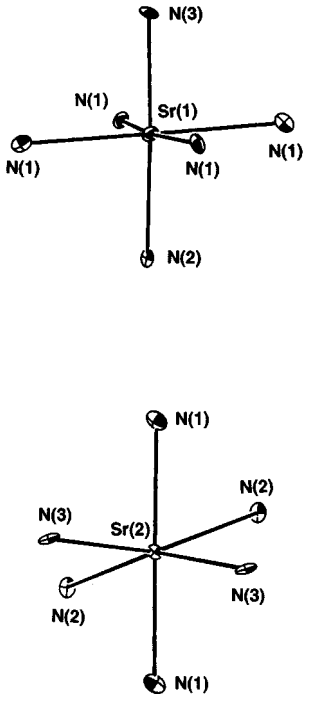

FIG. 3. Coordination environments of the Sr(1) and Sr(2) atoms in $Li_3Sr_2NbN_4$.

a temperature independent paramagnetism between 4 and 300 K (average $5.61(5) \times 10^{-3}$ emu/mol). Temperature independent paramagnetism ($\chi = 1.53 \times 10^{-4}$ emu/mol) was also reported for Ba_2NbN_3 between 20 and 300 K (11).

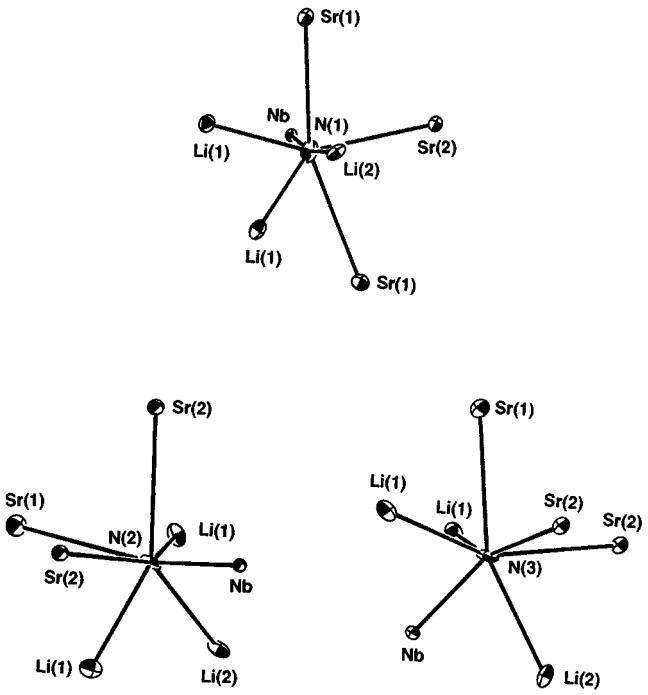

FIG. 4. Coordination environments of N atoms in $Li_3Sr_2NbN_4$.

ACKNOWLEDGMENTS

Assistance from Reza Loloee in obtaining the magnetic data and helpful suggestions from a referee are acknowledged gratefully.

REFERENCES

1. D. A. Vennos and F. J. DiSalvo, *J. Solid State Chem.* **98,** 318–322 (1992).
2. D. H. Gregory, M. G. Barker, P. P. Edwards, and D. J. Siddons, *Inorg. Chem.* **34,** 3912–3916 (1995).
3. D. A. Vennos and F. J. DiSalvo, *Acta Crystallogr.* **48,** 610–612 (1992).
4. Ch. Wachsmann and H. Jacobs, *J. Alloys Compound.* **190,** 113–116 (1992).
5. U. Zachwieja and H. Jacobs, *Eur. J. Solid State Inorg. Chem.* **28,** 1055–1062 (1991).
6. Th. Brokamp and H. Jacobs, *J. Alloys Compound.* **176,** 47–60 (1991).
7. Th. Brokamp and H. Jacobs, *J. Alloys Compound.* **183,** 325–344 (1992).
8. H. Jacobs and B. Hellmann, *J. Alloys Compound.* **191,** 277–278 (1993).
9. H. Jacobs and B. Hellmann, *J. Alloys Compound.* **191,** 51–52 (1993).
10. N. E. Brese and F. J. DiSalvo, *J. Solid State Chem.* **120,** 378–380 (1995).
11. O. Seeger, M. Hofmann, J. Strähle, J. P. Laval, and B. Frit, *Z. Anorg. Allg. Chem.* **620,** 2008–2013 (1994).
12. F. K.-J. Helmlinger, P. Höhn, and R. Kniep, *Z. Naturforsch. B* **48,** 1015–1018 (1993).
13. (a) X. Z. Chen and H. A Eick, *J. Solid State Chem.* **113,** 362–366 (1994). (b) X. Z. Chen, D. L. Ward, and H. A. Eick, *J. Alloys Compound.* **206,** 129–132 (1994).
14. X. Z. Chen, W. Lasocha, and H. A. Eick, manuscript in preparation.
15. A. Gudat, P. Höhn, R. Kniep, and A. Rabenau, *Z. Naturforsch. B* **46,** 566–572 (1991).
16. O. Seeger and J. Strähle, *Z. Anorg. Allg. Chem.* **621,** 761–764 (1995).
17. A. Tennstedt, C. Röhr, and R. Kniep, *Z. Naturforsch. B* **48,** 794–796 (1993).
18. A. Tennstedt, R. Kniep, M. Hüber, and W. Haase, *Z. Anorg. Allg. Chem.* **621,** 511–515 (1995).
19. D. A. Vennos, M. E. Badding, and F. J. DiSalvo, *Inorg. Chem.* **29,** 4059–4062 (1990).
20. G. R. Kowach and F. J. DiSalvo, Abstract No. 33, Division of Inorganic Chemistry, 210th ACS National Meeting, Chicago, August 20–24, 1995.
21. (a) H. Jacobs and B. Hellmann, *J. Alloys Compound.* **191,** 51–52 and 277–278 (1993). (b) H. Jacobs and E. von Pinkowski, *J. Less-Common Met.* **146,** 147–160 (1989). (c) D. Ostermann, U. Zachwieja, and H. Jacobs, *J. Alloys Compound.* **190,** 137 (1994). (d) H. Jacobs and R. Niewa, *Eur. J. Solid State Inorg. Chem.* **31,** 105–113 (1994).
22. A. Gudat, R. Kniep, and J. Maier, *J. Alloys Compound.* **186,** 339–345 (1992), and references therein.
23. P. Höhn and R. Kniep, *Z. Naturforsch. B* **47,** 434–436 (1992).
24. P. Höhn, S. Haag, W. Milius, and R. Kniep, *Angew. Chem. Int. Ed. Engl.* **30,** 831–832 (1991).
25. N. E. Brese and M. O'Keeffee, *J. Solid State Chem.* **87,** 134–140 (1990).
26. W. Lasocha and H. A. Eick, *J. Solid State Chem.* **75,** 175–182 (1988).
27. J. W. Visser, *J. Appl. Crystallogr.* **2,** 89–95 (1969).
28. P.-E. Werner, L. Eriksson, and M. Westdahl, *J. Appl. Crystallogr.* **18,** 367–370 (1985).
29. A. Boultif and D. Louër, *J. Appl. Crystallogr.* **24,** 987–993 (1991).
30. K. Yvon, W. Jeitschko, and E. Parthé, *J. Appl. Crystallogr.* **10,** 73–74 (1977).
31. N. Walker and D. Stuart, *Acta Crystallogr. A* **39,** 158–166 (1983).
32. G. M. Sheldrick, *in* "Crystallographic Computing 3" (G. M. Sheldrick, C. C. Kruger, R. Doddard, Eds.), pp. 175–189. Oxford Univ. Press, Oxford, UK, 1985.

33. D. T. Cromer and J. T. Waber, "International Tables for X-ray Crystallography," Vol. IV, Table 2.2 A, Kynoch, Birmingham, England, 1974.
34. "TEXSAN—TEXRAY Structure Analysis Package," Molecular Structure Corporation, The Woodlands, TX, 1985.
35. (a) C. Wachsmann and H. Jacobs, *Z. Kristallogr.* **211,** 477 (1996). (b) X. Z. Chen and H. A. Eick, *J. Solid State Chem.* **127,** 19–24 (1996).
36. "CRC Handbook of Chemistry and Physics, 76th Edition," pp. 4–66. 1995–1996.
37. R. Luge and R. Hoppe, *Z. Anorg. Allg. Chem.* **520,** 39–50 (1985).
38. J. Köhler and R. Hoppe, *Z. Anorg. Allg. Chem.* **495,** 7–15 (1982).
39. A. Rabenau and H. Schulz, *J. Less-Common Met.* **50,** 155–159 (1976).
40. D. W. Appleman, D. S. Handwerker, and H. T. Evans, "Program X-Ray," Geological survey, U. S. Department of the Interior, Washington, DC, 1966.
41. R. X. Fischer and E. Tillmanns, *Acta Crystallogr. C* **44,** 775–776 (1988).